COBEM 2023 27TH INTERNATIONAL CONGRESS OF MECHANICAL ENGENEERING

ABCM Brazilian Society of Mechanical Sciences and Engineering
27th ABCM International Congress of Mechanical Engineering
December 04-08, 2023, Florianópolis-SC, Brazil

COB-2023-0699
NUMERICAL ESTIMATION OF NONLINEAR SPECIFIC HEAT AND LASER BEAM WELDING (LBW) EFFICIENCY

Ariel Flores Monteiro de Oliveira
Elisan dos Santos Magalhães
Kahl Dick Zylnik
Instituto Tecnológico de Aeronáutica – ITA, 12228-900 São José dos Campos, SP.
arielafmo@ita.br; elisan@ita.br; zilnyk@ita.br.

Philippe Le Masson
Université de Bretagne-Sud – UBS, Rue de Saint Maudé, Lorient, France
philippe.le-masson@univ-ubs.fr

Abstract. *Several industrial processes are realized in high temperatures, i.e., temperatures close to the melting point, such as welding, additive manufacturing, and forging. Accurate computational simulation of these processes relies on selecting a precise thermal model and considering particular thermal properties. Such properties are strongly dependent on material composition and temperature. This work applied the Quadrilateral Optimization Method (QOM) to assess the SAE 1020 steel specific heat (c_p) and efficiency related to LASER beam welding (LBW) processing. The algorithm written in CUDA-C was adapted to estimate the three variables concurrently. The specific heat is an exponential temperature function with two coefficients to be assessed. The LASER efficiency is obtained by evaluating the gross heat rate, a constant value used for the heat input calculus. The QOM minimizes an objective function, subjected to the Future Time Regularization (FTR), to enhance sensibility. To perform FTR, a suitable number of time steps must be used. The optimum number is evaluated and applied in this work. The method is robust and sensitive enough to acquire such parameters. Also, the simulated temperature using reference and estimated values were compared and showed no significant deviations. Consequently, the QOM is suitable for simultaneously estimating the specific heat in function of temperature and the energy directed to the sample during LBW.*

Keywords: *thermal properties, numerical estimation, quadrilateral optimization method, GPU processing.*

1. INTRODUCTION

Simulations of numerical heat transfer problems require the definition of exact thermal properties for each studied material to correctly represent the physical interactions that occur in the sample. The implemented thermal properties are often nonlinear and vary with the temperature (Klimeš and Štětina, 2015; Manvatkar, De and DebRoy, 2015). However, the properties variation with the composition of the material, processing, and application hinders the cataloging of exact properties, mainly if high-temperature conditions are investigated (Zhao *et al.*, 2019).

It is possible to determine thermal properties such as thermal conductivity and specific heat capacity through experimental approaches. Nonetheless, interactions between metallic samples and their container may occur if the temperature is above the melting point of the metal (Lamien *et al.*, 2019). Hence, many techniques are suitable for measuring the properties of insulating materials (Jannot *et al.*, 2020; Kim, Lee and Yang, 2021) and may return specific properties at fixed temperature values (Somasundharam and Reddy, 2018) instead of a function valid for a temperature range.

The thermal properties for metals may be obtained by polynomial fitting of discrete data (Magalhães *et al.*, 2015) or based on data series, such as the Thermophysical Properties of Matter (TPRC) (Nishi *et al.*, 2003), though the values for molten metals being usually attained by extrapolating data for the respective solid material. This assumption may return non-exact property values, inducing errors in the simulations. The Flash Method is an appropriate experimental approach to studying metals at high temperatures, but the apparatus is often costly (Katz and Katz, 2017), and the methods frequently consider a small temperature range (Nishi *et al.*, 2003).

Hence, there are different numerical approaches to estimating thermal properties. It is possible to assess the thermal conductivity and the specific heat of different metal specimens by varying the heat flux intensity directed to a sample placed between a resistive heater and an insulator in a one-dimensional thermal model (Carollo, Lima e Silva and Lima e Silva, 2012). Magalhães (2021) developed the Quadrilateral Optimization Method (QOM) to estimate the two parameters of the specific heat capacity function varying with the temperature for SAE 1010. Indeed, the QOM could be applied to estimating the nonlinear thermal properties of materials in high temperatures.

In this work, the temperature distribution of a LASER beam welding (LBW) numerical experiment is obtained through an in-house algorithm written in CUDA-C that solves the three-dimensional heat diffusion equation through the finite volume method. The simulated temperature data is applied for assessing the specific heat in function of the temperature and the gross heat rate provided by the LASER using the Quadrilateral Optimization Method (QOM) developed by Magalhães (2021). The code was adapted to simultaneously estimate three parameters. The estimation procedure minimizes an objective function regulated by the Future Time Regularization (FTR) to add a temporal analysis and enhance QOM's sensitivity. Indeed, the number of time steps (*r*) affects the accuracy of the estimates. The optimum number of time steps required to perform the assessments was acquired by evaluating *r* ranging from 10 to 160. Moreover, a sensitivity analysis ensured that the results obtained using the QOM were reliable. Also, the method is robust for estimating such parameters since the results acquired using noisy data presented no significant deviation from the assessments that considered the reference temperatures. Hence, the Quadrilateral Optimization Method is a promising tool for acquiring the thermal properties of materials in a wide temperature range.

2. METHODS

2.1 Direct Thermal Model

The temperature profile is obtained using an in-house algorithm written in CUDA-C. The three-dimensional model is based on an autogenous LBW of SAE 1020. Such a welding process involves a high thermal gradient and significant peak temperatures. The nonlinear three-dimensional heat diffusion equation (Eq. (1)) defines the heat transfer and is solved through the finite volume method.

$$\frac{\partial}{\partial x}\left(\lambda(T)\frac{\partial T}{\partial x}\right)+\frac{\partial}{\partial y}\left(\lambda(T)\frac{\partial T}{\partial y}\right)+\frac{\partial}{\partial z}\left(\lambda(T)\frac{\partial T}{\partial z}\right)+\dot{g}=\frac{\partial H}{\partial t} \tag{1}$$

Where *x*, *y*, and *z* are the cartesian coordinates, $\lambda(T)$ is the nonlinear thermal conductivity, T is the numerical temperature, $\dot{g}$ is the generated heat source, t is the time, and H is the enthalpy function that describes the phase change process, given by:

$$H=(1-f)\int_0^{T_f}\rho c_{p,s}dT+f\int_{T_f}^{T}\rho c_{p,l}dT+\rho fL \tag{2}$$

where f is the Heaviside step function, T_f is the fusion temperature, ρ is the specific mass, $c_{p,s,}$ and $c_{p,l}$ are the nonlinear specific heat of the material in the solid and liquid states, respectively, and L is the latent heat of fusion.

In this case, the thermal properties are accounted for as temperature functions. The specific heat (c_p) function is exponential, composed of two real terms (ϕ_i) that vary with sample composition. In this case, the subscript i goes from 1 to 2. The function may be expressed as:

$$c_p=\phi_1\times10^2\times\exp(\phi_2\times10^{-3}T) \tag{3}$$

Moreover, the generated heat source follows the polynomial distribution described by (Magalhães *et al.*, 2018):

$$\dot{g}=\frac{\omega}{0.46hR^2}e^{-\frac{4.5(z-ut)^2}{R^2}}e^{-\frac{4.5(z-L_y/2)^2}{R^2}}\left(1-\frac{x^{1/2}}{h^{1/2}}\right) \tag{4}$$

where ω is the gross heat rate, h is the penetration coordinate, R is the welding radius, L_y is the sample width, and u is the welding velocity. The numerical values of 0.46 and 4.5 slightly modify the distribution proposed in (Magalhães *et al.*, 2015) to increase the similarity between experimental and numerical responses.

Additionally, the Eq. (4) parameters as h, R, and ω are obtained based on the experimental setup that conducted the modeling. However, such parameters must be calibrated to match numerical and experimental data (de Oliveira *et al.*, 2023). The gross heat rate (ω) defines the energy the LASER provides to the sample. Such power may be related to the process efficiency once the experimental heat source power configuration does not represent the amount of energy the sample absorbs. Generally, the LBW efficiency ranges from 76% to 87% (Tadamalle *et al.*, 2014; Fakir *et al.*, 2020). Indeed 79.5% of the power emitted by the LASER was absorbed by an SAE 1020 steel sample during LBW (da Silva *et al.*, 2023). In this case, ω=1000W. Further details about the algorithm development and thermal model may be found at (Magalhães et al., 2015, 2018; Magalhães, Silva and Silva, 2017).

2.2 The Quadrilateral Optimization Method (QOM)

The Quadrilateral Optimization Method (QOM) proposed by Magalhães (2021) was adapted to simultaneously assess the gross heat rate (ω) and the specific heat function for SAE 1020 steel. The use of the QOM for estimating parameters requires the definition of how many variables will be assessed (n_{var}), convergence rate (τ), relative tolerance (χ), the maximum number of interactions (φ), and upper ($\xi_{i,0}$) and lower ($\xi_{i,1}$) bounds for each variable, considering a general parameter ξ. $\xi_{i,0}$ and $\xi_{i,1}$ determine the limits of the search domain, which comprises all the possible linear combinations among the parameters.

Hereafter, the code sets an initial guess vector composed of 27 combinations. The objective function (F) is computed for each guess. The sensitivity of F is enhanced by minimizing it in a future time step rather than the present through the Future Time Regularization (FTR). The primary objective of the optimization method is to minimize the objective function expressed as,

$$F = \sum_{q=0}^{r} \sum_{m=0}^{n} (T'_{m,q} - T^{0}_{m,q})^2 \tag{5}$$

where r is the number of time steps adopted, q is related to the time step position, n is the number of sensors, m is the sensor number, T' is the numerical temperature, and T^0 is the reference temperature.

Then, for each guess vector, the point that presents the minor F becomes the pivot point (p), and the method defines 27 new combinations to be evaluated, equally distributed around the pivot point. The calculations continue until the maximum number of interactions is reached. The step-by-step of the QOM is outlined in Figure 1.

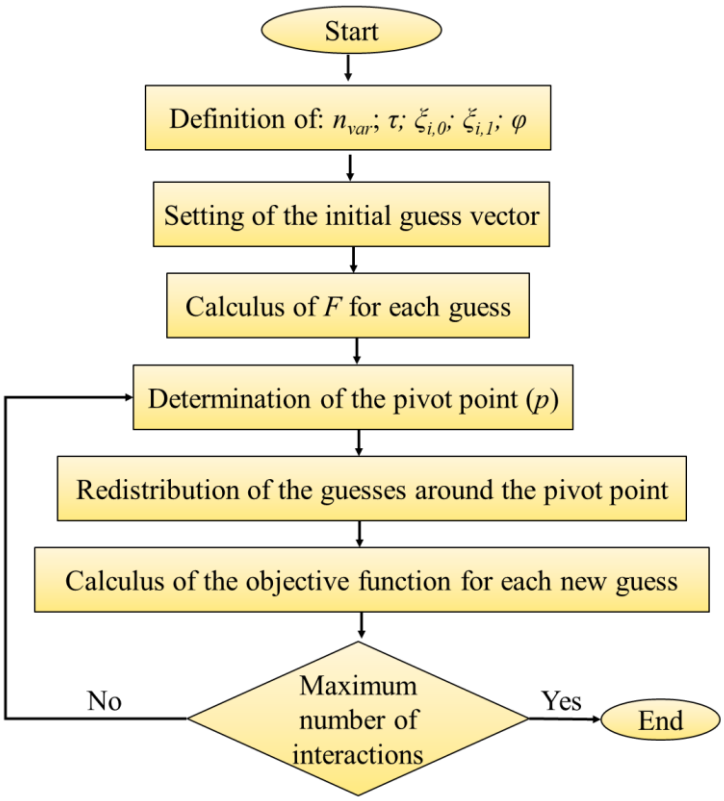

Figure 1. Step-by-step QOM procedure.

2.2.1 Definition of the evaluated parameters

The gross heat rate (ω) applied in the heat input calculus (Eq. (4)) is a constant parameter. Hence, a single value must be assessed. Furthermore, the aim values regarding the specific heat function are obtained from (Touloukian *et al.*, 1970). The aim values the method should find and the limits of the search domain are exhibited in Table 1.

Table 1. Goal values to be obtained through the QOM and search domain definition.

Variable	Goal value	Lower bound ($\xi_{i,0}$)	Upper bound ($\xi_{i,1}$)
ϕ_1	3.30×10^2	3.00×10^2	4.00×10^2
ϕ_2	1.509×10^{-3}	1.000×10^{-3}	2.000×10^{-3}
ω [W]	1000	500	1500

2.3 Time-steps evaluation

Standardizing the objective function through the FTR adds a temporal factor to the analysis. According to Eq. (5), the number of time steps (r) used in the estimations affects the sensitivity of the objective function. Also, the number of time steps is proportional to the computational time spent on the simulations. The number of iterations is constant. However, more or less time steps may be considered in each iteration.

This work calculated the average F values using 100 to 1500 time steps. The average value is obtained by the ratio of F to the number of time steps. It is necessary to use such an average so the results are comparable.

2.4 QOM suitability for assessing the specific heat and LASER gross heat rate

The scaled sensitivity coefficients (S) of the temperature related to each parameter were obtained to verify whether the method is sensitive enough to acquire such ω, ϕ_1, and ϕ_2. This work acquires the temperature at nine distinct spots. Hence, it is necessary to sum the coefficients of all sensors. The sensitivity coefficient for multiple sensors is represented by:

$$S = \sum_{n=1}^{Nt} \xi \frac{\partial T}{\partial \xi} \tag{6}$$

where n is the sensor number, Nt is the total number of sensors, in this case, 9, and ξ is the investigated parameter.

The sensitivity coefficients determine how significant the temperature oscillation is due to a parameter variation. A 0.1% increase is evaluated. The greater the sensitivity coefficient, the more reliable the assessments are.

Furthermore, the temperatures acquired by the direct model are algorithm inputs used as start points for the estimates. The closer the predicted temperature to the reference data (input), the lesser the F. The robustness of the method was evaluated by adding random errors to the temperature data, representing a 5% standard deviation (σ) from the reference temperatures. Then, the estimations were performed using the disturbed data. If the method is robust enough, no deviations over 5% must be found for any assessed parameter.

3. OPTIMAL NUMBER OF TIME STEPS

Indeed, the objective function is different if distinct numbers of time steps are studied. F is below 0.3 for every r considered, as exhibited in Figure 2. Hence, the method could reach temperature values close to the reference data in the studied r range. If only the minimum value of F was pondered, the estimations could consider 100, 1200, 1400, or 1500 future time steps as the F under such conditions are the closest to 0.

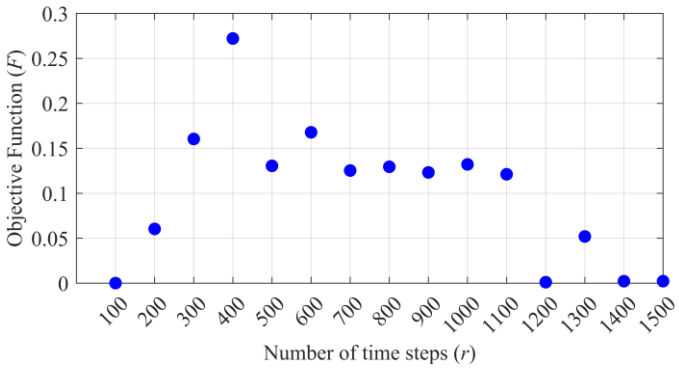

Figure 2. Oscillation of the objective function related to the number of time steps adopted in the TTR.

However, using fewer time steps in the calculus is advisable to reduce the computational time. Hence, the deviation from the estimated to goal values was evaluated through the percentage error. More significant deviations were found for

every parameter evaluated when considering 100 and 200 points, decreasing significantly from 300. Indeed, the error percentages for the assessment using 100 and 200 points are significantly high. The errors for ϕ_1, ϕ_2, and ω are shown in Table 2. Thus, the specific heat function and the gross heat rate were estimated using 300 points, corresponding to the configuration with lesser r and negligible errors.

Table 2. Error percentages for ϕ_1, ϕ_2, and ω for r ranging from 100 to 1500.

r	ϕ_1	ϕ_2	ω
100	5.18	12.57	16.41
200	4.07	7.96	7.14
300	0.21	0.29	0.00
400	0.28	0.35	8.90×10^{-2}
500	1.47×10^{-2}	8.72×10^{-2}	3.60×10^{-2}
600	0.26×10^{-2}	8.72×10^{-2}	4.50×10^{-2}
700	0.23×10^{-2}	8.22×10^{-2}	4.70×10^{-2}
800	1.67×10^{-2}	9.74×10^{-2}	0.04
900	0.58×10^{-2}	9.89×10^{-2}	0.03
1000	8.48×10^{-2}	7.86×10^{-2}	0.00
1100	0.30×10^{-2}	9.28×10^{-2}	0.04
1200	0.03×10^{-2}	0.01×10^{-2}	0.00
1300	9.24×10^{-2}	0.12	0.02
1400	0.15×10^{-2}	0.01×10^{-2}	0.00
1500	0.03×10^{-2}	0.22×10^{-2}	0.00

4. SENSITIVITY ANALYSES

The sensitivity coefficients of ϕ_1, ϕ_2, and ω with respect to time are displayed in Figure 3. S is close to 0 from the beginning of the experiment until circa 0.34 seconds. This behavior may be justified because the temperature increase is nonsignificant at this period. However, S assumes expressive values from this point. The maximum S for ω is 1064 at circa 0.5 seconds. At the same time, both specific heat function parameters present a peak. However, higher S are found from 2 seconds for ϕ_1, ϕ_2. It corresponds to the experiment time when the sample is cooling. As the coefficients are significant for every parameter evaluated, the estimations should be accurate.

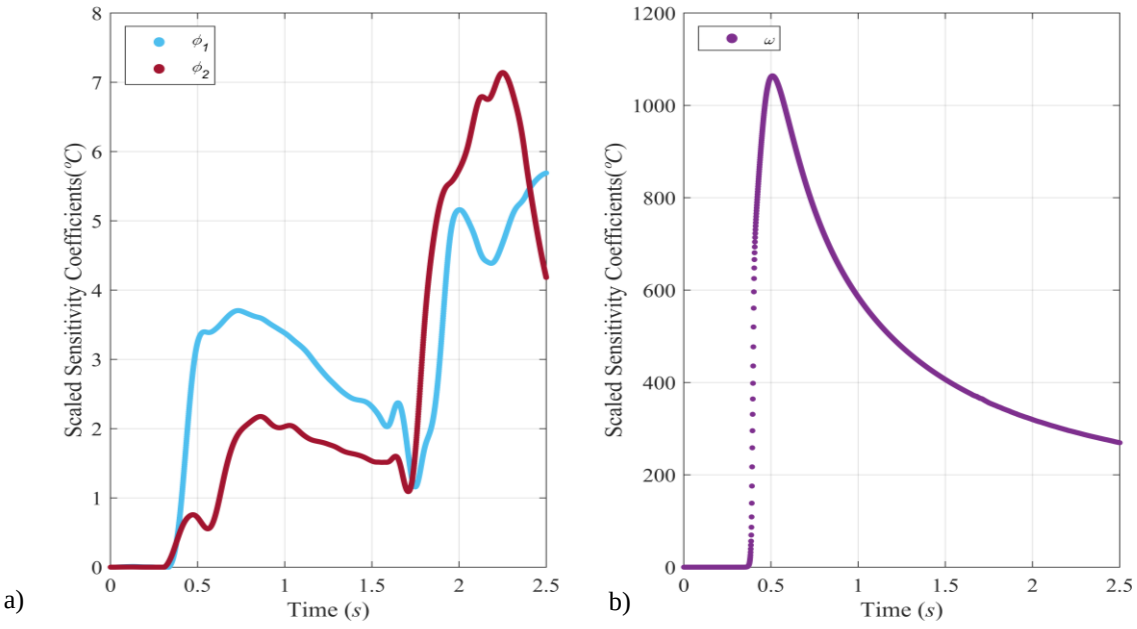

Figure 3. Scaled Sensitivity coefficients. a) Specific heat coefficients (ϕ_1, ϕ_2). b) Gross heat rate (ω).

The sensitivity coefficients may vary if the experimental set is altered. For instance, the heat flux intensity, time for data acquisition, and sensor positioning may affect the *S*. One may determine the optimal experimental design for parameter estimation by varying such parameters (Taktak, Beck and Scott, 1993). However, the significant coefficients shown in Figure 3 express no need to adapt any model parameter for the studied condition.

.

5. QOM'S ROBUSTNESS

Normally distributed errors representing a 5% standard deviation (σ) were added to the reference temperatures to investigate if the QOM is robust enough to estimate the specific heat function and LASER power under the studied conditions. The QOM results for ϕ_1, ϕ_2, and ω acquired from the disturbed data are shown in Table 3. Indeed, the error percentages regarding the assessments performed using the reference and noisy data are negligible. No parameter presented deviations greater than 5%. This fact confirms that the QOM is robust enough to perform such estimates.

Table 3. QOM results for ϕ_1, ϕ_2, and ω assessments using disturbed data (5% of σ).

Variable	ϕ_1	ϕ_2	ω
Estimated: reference	3.30×10^{2}	1.505×10^{-3}	1000.00
Estimated: σ=5%	3.30×10^{2}	1.505×10^{-3}	1000.31
Absolute error (%)	9.08×10^{-4}	1.99×10^{-3}	3.10×10^{-2}

6. ASSESSMENTS

Regarding the nonlinear specific heat, only variables ϕ_1 and ϕ_2 must be minimized to attain the complete exponential function demonstrated in Eq.(3). Thus, the QOM is applied to assess ω along with the two other parameters. The comparison between the specific heat function assessed using 300 future time steps and the reference data is shown in Figure 4, for temperatures from 0 to 1300ºC. The estimated function matches the reference data.

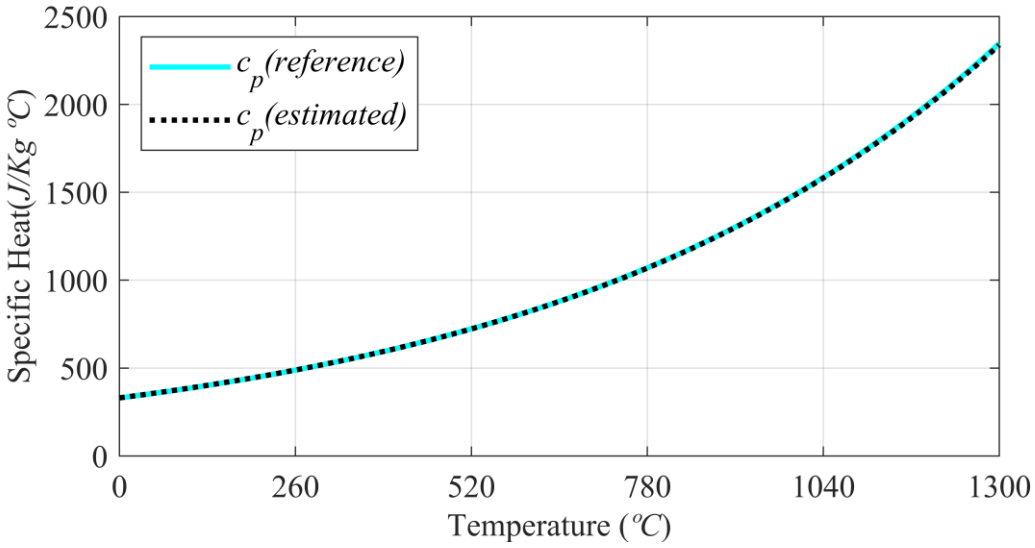

Figure 4. Nonlinear specific heat for SAE 1020 steel.

Moreover, the temperature profiles computed using the reference (red solid line) and the estimated parameters (black dashed line) for all sensors are shown in Figure 5. The sensors are positioned with a 1 mm deviation from each other along the *y*-axis. As the dots lie above the curves for the respective positions, the slight deviations in the assessments do not represent significant variations in the predicted temperatures. Hence, the QOM could be successfully applied to acquire the gross heat rate, i.e., the LASER power and the nonlinear specific heat function.

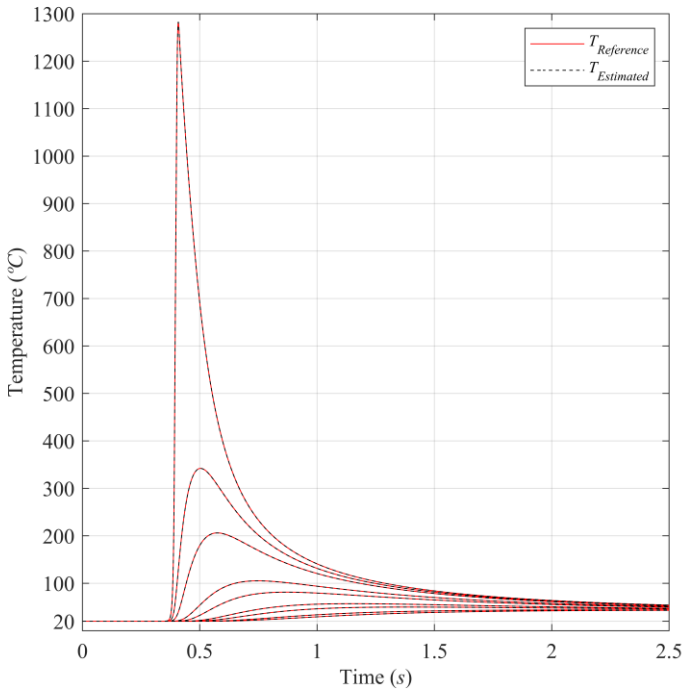

Figure 5. Computed temperature using reference and estimated data.

7. CONCLUSIONS

This work used the Quadrilateral Optimization Method (QOM) to simultaneously estimate the nonlinear specific heat function and the heat rate provided by the source in a numerical LASER beam welding (LBW) experiment. The algorithm minimizes an objective function, which is regularized by the FutureTime Regularization (FTR) to enhance QOM's sensitivity by accounting for temporal analysis. The number of time steps (r) used in the calculus was evaluated. Variations in r led to less or more accurate estimations. The optimum r that required the least computational time and acceptable error percentages is 300.

Moreover, the suitability of the method for assessing the thermal property and the LASER power was investigated through a sensitivity analysis. The calculated sensitivity coefficients are high enough to corroborate that the appraisements are trustable. Also, the robustness of the methodology was examined by adding normally distributed errors on the temperature data, representing a 5% standard deviation. The temperature acquired through the direct thermal model of the experiment is the baseline for the appraisements. Hence, the noisy data replaced the reference data, and the QOM was applied to perform the estimates. There were no significant deviations for any parameter assessed, confirming that the method is robust enough to perform the calculations.

Therefore, the QOM was successfully applied to assess the exponential specific heat function parameters related to the temperature and the heat input directed to the sample by the LASER source. Using a parallel computing algorithm requires little computational time to perform the calculations to solve the inverse problem.

8. ACKNOWLEDGEMENTS

The authors acknowledge CAPES, PETROBRAS and FUNDEP for their financial support.

9. REFERENCES

Carollo, L.F.S., Lima E Silva, A.L.F. and Lima E Silva, S.M.M. (2012) 'Applying different heat flux intensities to simultaneously estimate the thermal properties of metallic materials', *Measurement Science and Technology*, 23, p. 065601. Available at: https://doi.org/10.1088/0957-0233/23/6/065601.

Fakir, R. *et al.* (2020) 'Analysis of the Mechanical Behavior of AISI 4340 Steel Cylindrical Specimens Heat Treated with Fiber Laser', *Journal of Manufacturing Processes*, 55, pp. 41–56. Available at: https://doi.org/10.1016/j.jmapro.2020.03.039.

Jannot, Y. *et al.* (2020) 'A Comparative Fluxmetric (CFM) Method for Apparent Thermal Conductivity Measurement of Insulating Materials at High Temperature', *International Journal of Thermophysics*, 41(7), pp. 1–15. Available at: https://doi.org/10.1007/s10765-020-02676-x.
Katz, M.D. and Katz, I.M. (2017) 'Evaluation of the laser-flash method and its errors for determining of materials thermal diffusivity at high temperatures', *MATEC Web of Conferences*, 110, pp. 4–8. Available at: https://doi.org/10.1051/matecconf/201711001037.
Kim, D., Lee, S. and Yang, I. (2021) 'Verification of thermal conductivity measurements using guarded hot plate and heat flow meter methods', *Journal of the Korean Physical Society*, 78(12), pp. 1196–1202. Available at: https://doi.org/10.1007/s40042-021-00177-0.
Klimeš, L. and Štětina, J. (2015) 'A rapid GPU-based heat transfer and solidification model for dynamic computer simulations of continuous steel casting', *Journal of Materials Processing Technology*, 226, pp. 1–14. Available at: https://doi.org/10.1016/j.jmatprotec.2015.06.016.
Lamien, B. *et al.* (2019) 'A Bayesian approach for the estimation of the thermal diffusivity of aerodynamically levitated solid metals at high temperatures', *International Journal of Heat and Mass Transfer*, 141, pp. 265–281. Available at: https://doi.org/10.1016/j.ijheatmasstransfer.2019.06.054.
Magalhães, E. dos S. *et al.* (2015) 'The use of non-linear inverse problem and enthalpy method in GTAW process of aluminum ☆', *International Communications in Heat and Mass Transfer*, 66, pp. 114–121. Available at: https://doi.org/10.1016/j.icheatmasstransfer.2015.05.023.
Magalhães, E. dos S. *et al.* (2018) 'A thermal analysis in laser welding using inverse problems', *International Communications in Heat and Mass Transfer*, 92, pp. 112–119. Available at: https://doi.org/10.1016/j.icheatmasstransfer.2018.02.014.
Magalhães, E. dos S. (2021) 'A quadrilateral optimization method for non-linear thermal properties determination in materials at high temperatures', *International Journal of Heat and Mass Transfer*, 181, p. 121857.
Magalhaes, E. dos S., Silva, A.L.F. de L. e and Silva, S.M.M.L. e (2017) 'A GTA Welding Cooling Rate Analysis on Stainless Steel and Aluminum Using Inverse Problems', *Applied Sciences*, 7(122), p. 15. Available at: https://doi.org/10.3390/app7020122.
Manvatkar, V., De, A. and DebRoy, T. (2015) 'Spatial variation of melt pool geometry, peak temperature and solidification parameters during laser assisted additive manufacturing process', *Materials Science and Technology (United Kingdom)*, 31(8), pp. 924–930. Available at: https://doi.org/10.1179/1743284714Y.0000000701.
Nishi, T. *et al.* (2003) 'Thermal conductivities of molten iron, cobalt, and nickel by laser flash method', *Metallurgical and Materials Transactions A: Physical Metallurgy and Materials Science*, 34(12), pp. 2801–2807. Available at: https://doi.org/10.1007/s11661-003-0181-2.
de Oliveira, A.F.M. *et al.* (2023) 'A Thermal Analysis of LASER Beam Welding Using Statistical Approaches', *Processes*, 11(7), p. 25.
da Silva, R.G.D. *et al.* (2023) 'Estimating the absorption efficiency in a laser welding process using a nonlinear inverse problem method', *International Journal of Thermal Sciences*, 183(January 2022), p. 107846. Available at: https://doi.org/10.1016/j.ijthermalsci.2022.107846.
Somasundharam, S. and Reddy, K.S. (2018) 'Simultaneous estimation of thermal properties of orthotropic material with non-intrusive measurement', *International Journal of Heat and Mass Transfer*, 126, pp. 1162–1177. Available at: https://doi.org/10.1016/j.ijheatmasstransfer.2018.05.061.
Tadamalle, A.P. *et al.* (2014) 'Evaluation of Nd: YAG Laser Welding Efficiencies for 304L Stainless Steel', in *Procedia Materials Science*. Elsevier, pp. 1731–1739. Available at: https://doi.org/10.1016/J.MSPRO.2014.07.160.
Taktak, R., Beck, J. V. and Scott, E.P. (1993) 'Optimal experimental design for estimating thermal properties of composite materials', *International Journal of Heat and Mass Transfer*, 36(12), pp. 2977–2986. Available at: https://doi.org/10.1016/0017-9310(93)90027-4.
Touloukian, Y.S. *et al.* (1970) *Thermophysical properties of matter - the TPRC data series. Volume 1. Thermal Conductivity Metallic Elements and Alloys*. 1st edn. New York.
Zhao, S. *et al.* (2019) 'Simultaneous retrieval of high temperature thermal conductivities, anisotropic radiative properties, and thermal contact resistance for ceramic foams', *Applied Thermal Engineering*, 146, pp. 569–576. Available at: https://doi.org/10.1016/j.applthermaleng.2018.10.021.

10. RESPONSIBILITY NOTICE

The authors are the only responsible for the printed material included in this paper.